NUMERICAL AND EXPERIMENTAL INVESTIGATION OF DIMENSIONAL ACCURACY IN INCREMENTAL FORMING OF AA6063 TUBES

Seyed Jalal Hashemi[1], Farzad Rahmani[2], Seyed Mohammad Hossein Seyedkashi[3]

[1] Technical and Vocational University (TVU), Faculty of Enghelab-e Eslami, Department of Mechanical Engineering
Tehran 13715-173 Iran
[2] Kar higher Education Institute, Department of Mechanical Engineering
Qazvin, Iran
[3] University of Birjand, Faculty of Engineering, Mechanical Engineering Department
Birjand 97175-376, Iran

Corresponding author: Seyed Mohammad Hossein Seyedkashi, seyedkashi@birjand.ac.ir

Abstract: In the incremental tube forming process, a tool forms a desired shape on a tube by applying local force on a predetermined path. A rotating tool produces a symmetric bulge in the central region of AA6063 aluminum tubes. The forming process has been carried out in several steps and the final profiles of the components have been studied. The process is repeated to achieve the desired bulge height. The effects of process parameters are investigated on the spring-back and final tube length. The process is simulated using Abacus and the numerical results have shown good agreement with the experiments. The results show that the reduction of the axial pitch and the forming depth increases the plastic strain resulting in less spring-back. Tool velocity does not have a significant effect on the final diameter. By choosing the least forming depth and highest axial pitch, minimum change occurs along the tube.
Key words: incremental tube forming; spring-back; axial pitch; forming depth

1. INTRODUCTION

The idea of incremental forming was discussed by Leszac (1967). In this process, the raw material, which is usually a sheet metal is clamped by a blank-holder and gradually takes the final desired shape by means of a forming tool moving on a predetermined path (Martins et al., 2008). The tool movement is usually controlled by CNC machines. The incremental forming process greatly reduces the production costs and can be used in batch production and prototyping (Khalifa and Thiery, 2019).

In recent years, many researchers have worked on increasing the dimensional accuracy of the incrementally formed products. Most of them focused on the tool path strategy, tool shape and dimensions, and the sheet clamping mechanism. Ambrogio et al. (2004) investigated the effect of tool diameter and forming pitch on the formed wall angle. Micari et al. (2007) investigated the dimensional and shape accuracy in the single-point incremental forming of pyramids. According to their results, to increase the dimensional accuracy, the forming region should have the least distance from the clamping system. Attanasio et al. (2006; 2008) performed path optimization of the forming tool to improve the surface quality and dimensional accuracy. Ham and Ham and Jeswiet (2008) used the Box-Benken design to investigate the effect of parameters such as sheet thickness, tool diameter and forming pitch on dimensional accuracy. Behera et al. (2011; 2013) used a classification method to improve dimensional accuracy based on the interactions of the process parameters. They could reduce the dimensional accuracy error up to 0.4 mm by compensating the tool path error. Lingam et al. (2016) developed an analytical method to predict the displacement of the formed wall, and determine the precise forming path. This prediction was based on the tool diameter, forming depth and sheet thickness. Malhotra et al. (2012) developed a model to predict fracture in incremental forming process accurately. They implemented this model in finite element analysis.

Spring-back is a phenomenon that occurs after the forming process due to the elasticity of the material, and reduces the dimensional accuracy of the final product. It usually occurs in the incremental forming process, and is one of the main reasons for the dimensional inaccuracy. In incremental forming, due to the local contact of the tool with the sheet, the areas not in touch with the tool do not tolerate plastic deformation, and cause the spring-back at the contact area (Bambach, 2008). Duflou et al. (2007) used laser local heating at the tool contact point to increase dimensional accuracy. According to their results, the amount of spring-back in the heated area is reduced by stress reduction. Bamach et al. (2009) showed that the incremental forming process reduces the forming forces and so the amount of spring–back. According to Asghar et al. (2014), tool deviation and spring-back are the most important factors affecting the dimensional error of the formed piece. By compensating these two factors, they were able to significantly improve dimensional accuracy during the process.

Single-point incremental forming can be used as a die-less process to make various cross-sections on metal tubes. This process is called incremental tube forming (ITF). In this process, a rotating tool creates the final shape by applying force to the inner or outer wall of the tube along a forming path controlled by a CNC milling machine. Since the tubes with desired cross-sections are usually formed by the tube hydroforming process (Seyedkashi et al., 2012a and 2012b), the proposed method can reduce the limitations and drawbacks of hydroforming such as the need for high pressures, sealing problems and production costs. A few studies are published on incremental tube forming. Taramae et al. (2007) used incremental forming to create a flange on a tube. A hole was drilled on the tube wall and then flanged by incremental forming. The results showed that the thickness distribution of the formed flange is improved by increasing the strength hardening coefficient of the material. Yang et al. (2014) also investigated the flange forming in the tube and investigated the effect of tube diameter, shape and size of the initial hole on the dimensions of the flange. Tong et al. (2015) investigated the forming of four different shapes on the tube by incremental forming process. According to their results, the elastic deformation comprises a large part of the total deformation, which results in a significant spring-back. Raujol-Veillé et al. (2015) studied the numerical and experimental incremental flange forming at the edge of a steel tube, and showed that the concave geometry of the edge could reduce the spring-back. Seyedkashi et al. (2017) performed free expansion of copper tubes using incremental tube forming, and investigated the effect of process parameters on the thickness distribution and surface roughness of the product. Movahedinia et al. (2018) carried out the conical and pyramidal expansion of the edge of aluminum tubes using incremental forming. It was found that the higher cone angle was achievable compared with the press forming. Rahmani et al. (2019) experimentally studied the tube incremental forming in order to convert copper circular tubes into square cross-sectional parts. Cristino et al. (2020) have been used incremental forming process for plastic deformation at the end of aluminium tubes.

Since the tool path is easily programmable on the CNC machine, it is possible to produce various cross-section shapes on the tubes using the ITF process. In this research, the axisymmetric bulging of the central region of an AA6063 aluminum tube has been numerically and experimentally investigated. Due to the low formability of the material, multi-stage forming is used. At each stage, a certain amount of expansion has occurred in the tube. As mentioned above, one of the main problems of the incremental forming is dimensional inaccuracy due to the spring-back phenomenon which is addressed in this paper. In this regard, the specimens are formed under various process conditions, and their outer profiles are investigated to find the precise selection of these parameters in order to achieve the highest accuracy.

2. METHODOLOGY

The experimental setup used in this research is shown in Figure 1(a). The tube is fixed at its two ends by two upper and lower dies that conform to the outer surface of the tube. The forming tool has a specific tip radius which is shown in Figure 1(b). During the first forming pass, the tool contacts the inner surface of the tube at the desired start point at the free zone between the dies, and moves in a radial direction to deform it. This amount of the tool radial displacement is called "forming depth" (D). Then, it rotates a full circle around the tube axis, and continues with a spiral movement towards the end of the desired forming region. The downward spiral pitch of the tool is called "axial pitch" (P). At the end of the forming zone, the tool performs another complete circular movement to increase the corner radius accuracy. After the first pass, the tool returns to the start point rapidly. If a higher bulge is required, the tool moves radially again according to the forming depth. This procedure is repeated until the desired outer diameter of the tube (bulge height) is achieved. Tool linear velocity (V) is constant during the forming.

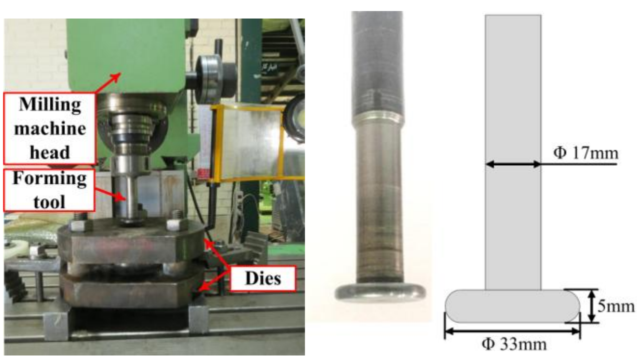

(a) (b)

Fig. 1. (a) Die setup on CNC milling machine, (b) Forming tool geometry

The overall length of the tube is 60mm. 18mm of each end is in contact with the dies, and limits the tube axial movement by friction force.
All movements of the forming tool are programmed by the G-codes defined in a CNC milling machine. Obtaining of an exact outer diameter is not possible without considering the spring-back phenomenon and the thickness changes during the forming. The aluminum tubes used in this research are AA6063 alloy with an outer diameter of 40mm and thickness of 1.5mm. The engineering stress-strain curve of the tube shown in Figure 2 is obtained by standard tensile test according to ASTM-E8M.

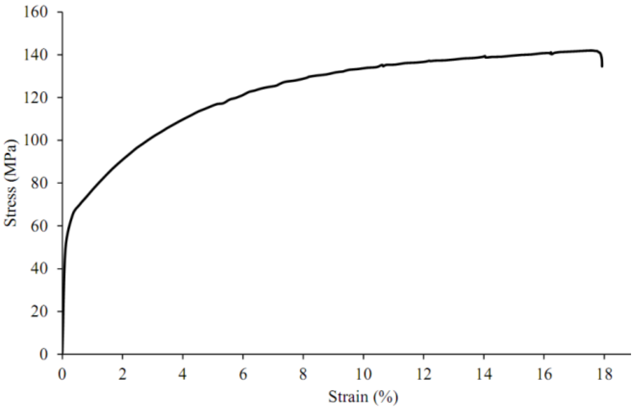

Fig. 2. Aluminum tube stress-strain curve

Abaqus/implicit software is used to simulate the incremental tube forming process of aluminum tubes. The tool path is defined according to the experimental section. The top and bottom dies are modeled as analytical rigid, while the forming tool is discrete rigid. The aluminum tube is modeled as a shell with 1830 elements of S4R mesh type. The coefficient of friction between the tube surface and the tooling is assumed to be 0.1. The plastic properties of the tubes were computed according to the results of the tensile test. The von-Mises yield function was used with the isotropic hardening model. In order to accurately determine the effect of tool velocity, the forming time in the simulation is equal to the real experimental time. Design of experiments (DOE) was used based on the full factorial method to study the effect of process parameters on spring-back and thickness distribution. The effective factors and their related levels are shown in Table 1. The controllable dimensional parameter during the forming is the tube outer diameter. However, this diameter is decreased after forming due to the spring-back. In all simulations, the number of forming passes is selected in a way that the theoretical bulge diameter after the last pass is 50 mm. In this way, it would be possible to determine the effect of the process parameters on the dimensional accuracy after measuring the actual dimensions.

Table 1. Design of experiments table

Factor	Forming depth, D [mm]	Axial pitch, P [mm]	Linear velocity, V [mm/min]
levels	0. 5 0. 75 1 1. 25	0. 5 0. 75 1 1. 25	400 800

3. RESULTS AND DISCUSSION

3.1 Validation of Finite Element Model

Figure 3 shows the strain distribution at the end of different forming passes with the forming depth and axial pitch of 1.25mm at 800mm/min. As the tool is fed into the tube, the plastic strain and the bulge diameter increase.

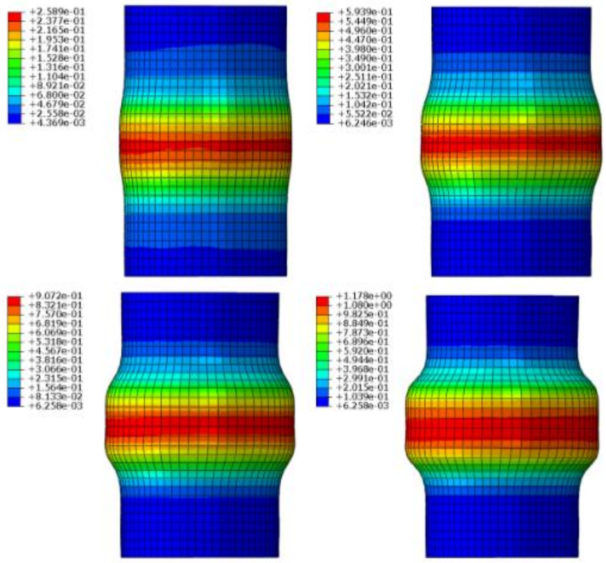
Fig. 3. Distribution of plastic strain at the end of forming passages with a forming depth and axial pitch of 1.25mm at 800mm/min

Four specimens formed under different process conditions are shown in Figure 4. The thickness distribution along the longitudinal line in two different states for the effective parameters are shown in Figure 5. As can be seen in Figure 5, the minimum thickness is created in the upper corner of the product, where the radial penetration of the tool at each pass occurs. In this area, the tube is involved on one side of the tool contact with the die, and its displacement is restricted resulting in greater tension on the tube wall. A 5% deviation is seen between the numerical and experimental results which is acceptable. The outer surface profiles of the specimens were also measured, and the diameter at different points along the specimen was compared with the numerical results in Figure 6. In the case of the profiles, also a good agreement between the numerical and experimental results is obtained.

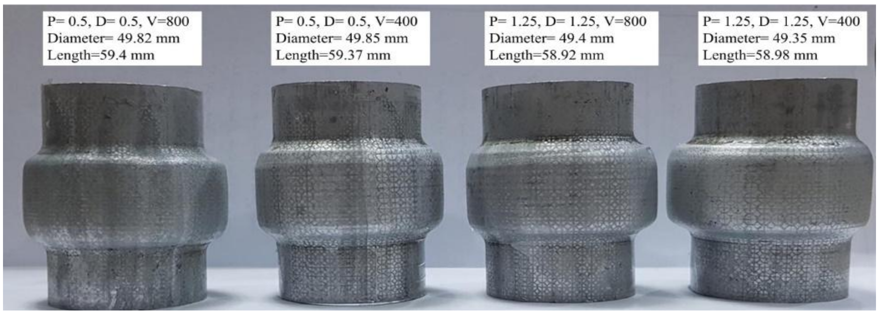

Fig. 4. Formed products

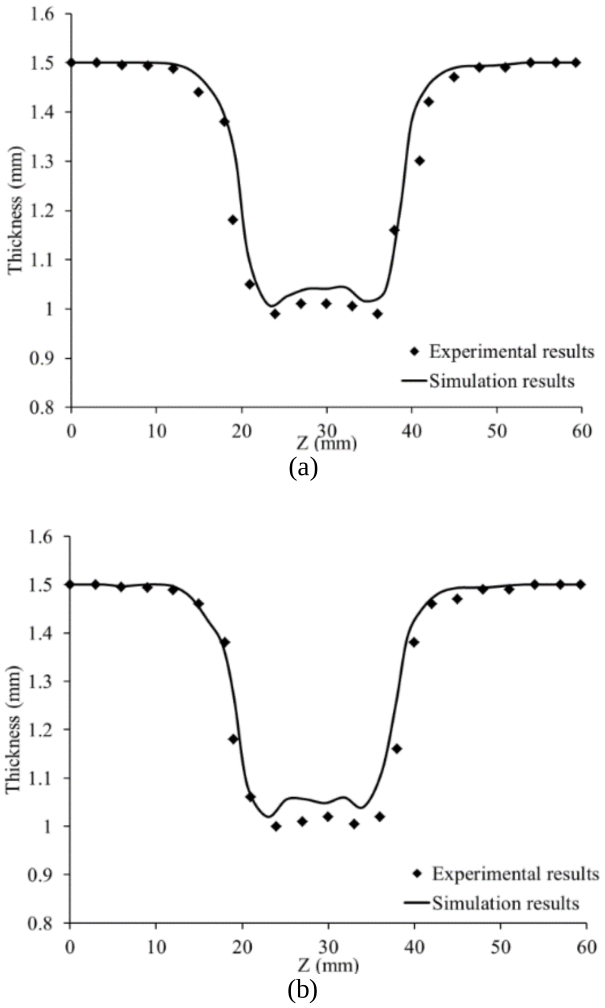

Fig. 5. Thickness distribution along the axial direction; (a) P=0.5, D=0.5, V=800, (b) P=1.25, D=1.25, V=400

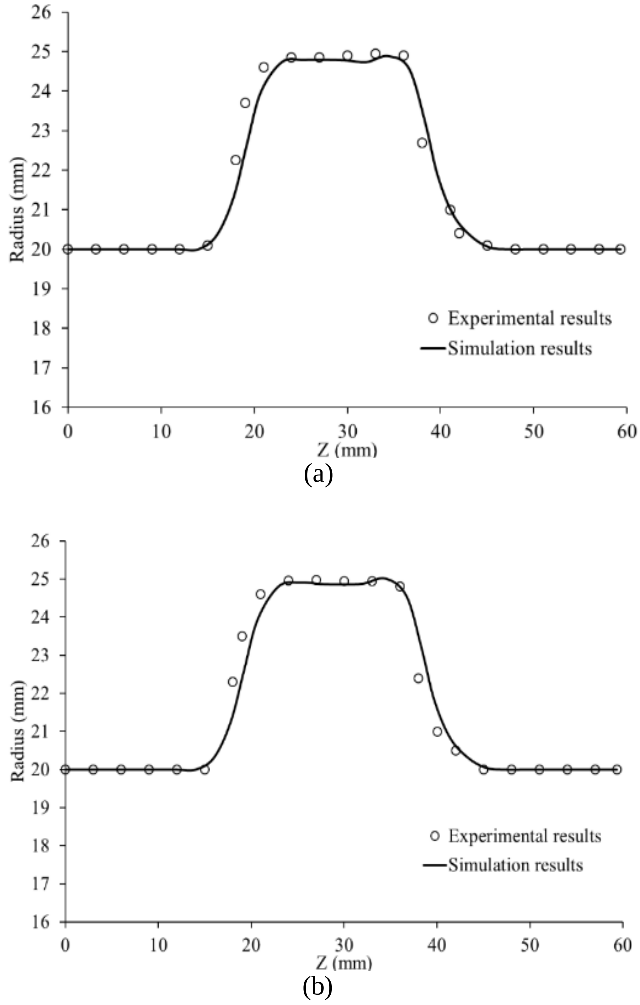

Fig. 6. External surface profiles of specimens; (a) P=0.5, D=0.5, V=800, (b) P=1.25, D=1.25,V=400

3.2 Dimensional Accuracy

After numerical simulation of incremental forming of aluminum tubes, in order to investigate the effect of input parameters on the dimensional accuracy, the diameters of the tubes in their middle length were measured. The results are shown in Table 2. Due to the spring-back, the diameter of all parts is less than the amount that was imposed by the tool movement at the last pass. On the other hand, the length of the specimens is less than the initial value due to the material flow into the forming area. The maximum diameter (minimum spring-back) is obtained with a 0.5 mm axial pitch and forming depth.

Table 3 shows the contribution percentage of the effect of each parameter on the bulge diameter and tube length. The forming depth has the highest contribution on these responses. Its effect on bulge diameter and tube length is 97.82% and 86.88%, respectively. According to the results, the tool linear velocity has no significant effect on the results. This may be related to the insensitivity of the material to the strain rate at ambient temperature. On the other hand, the effect of the axial pitch on the tube length is more than the formed diameter. The interaction effect of the forming depth and axial pitch on the length of the specimen is also significant.

Table 2. Actual diameter and length of formed specimens

No.	Axial pitch, P (mm)	Forming depth, D (mm)	Velocity, V (mm/min)	Diameter (mm)	Length (mm)
1	0.5	0.5	400	49.89	59.35
2	0.75	1.25	400	49.46	58.6
3	0.75	0.75	800	49.75	59.13
4	1	0.75	400	49.72	59.24
5	0.5	1	800	49.6	58.83
6	1.25	1.25	400	49.39	58.9
7	0.5	0.75	800	49.76	59.09
8	0.75	0.5	800	49.86	59.39
9	1.25	1.25	800	49.46	58.89
10	1	1.25	800	49.47	58.75
11	1.25	0.5	400	49.84	59.44
12	0.5	0.75	400	49.74	59.09
13	1.25	1	400	49.57	59.13
14	0.75	0.5	400	49.86	59.4
15	1	1.25	400	49.41	58.77
16	0.75	1	800	49.59	58.86
17	1	1	400	49.61	58.99
18	0.5	1.25	400	49.45	58.58
19	0.5	0.5	800	49.89	59.34
20	0.75	0.75	400	49.73	59.14
21	0.75	1	400	49.62	58.86
22	0.5	1.25	800	49.48	58.59
23	1	0.5	800	49.86	59.44
24	1.25	1	800	49.56	59.11
25	1.25	0.5	800	49.84	59.41
26	1	0.5	400	49.85	59.45
27	1.25	0.75	400	49.71	59.35
28	1	1	800	49.58	59
29	1	0.75	800	49.74	59.24
30	0.5	1	400	49.63	58.82
31	1.25	0.75	800	49.7	59.34
32	0.75	1.25	800	49.47	58.6

Table 3. Contribution of parameters on the bulge diameter and tube length

Parameters	Contribution on bulge diameter, %	Contribution on tube length; %
Forming depth (D)	97. 82	86. 88
Axial pitch (P)	1. 21	11. 04
Linear velocity (V)	0. 07	0. 01
Forming depth×Axial pitch (D×P)	0. 6	2. 03

The main effect of the factors on the bulge diameter is shown in Figure 7. According to this figure, the bulge diameter decreases with increasing the forming depth and axial pitch, i.e. larger spring-back has occurred. The plastic strain distribution along the tube length for four different levels of axial pitch with a forming depth of 1.25mm and a velocity of 800 mm/min is shown in Figure 8(a). Accordingly, by decreasing the axial pitch, the amount of plastic strain in the forming region, especially in the middle of the tube will increase, resulting in a lower spring-back and an increased bulge diameter. At any time during the forming in the tool/tube contact area, the tube wall undergoes simultaneous bending and tensile deformation. As the axial pitch increases, the non-contact parts of the tube will experience less plastic deformation, and eventually create a larger spring-back.

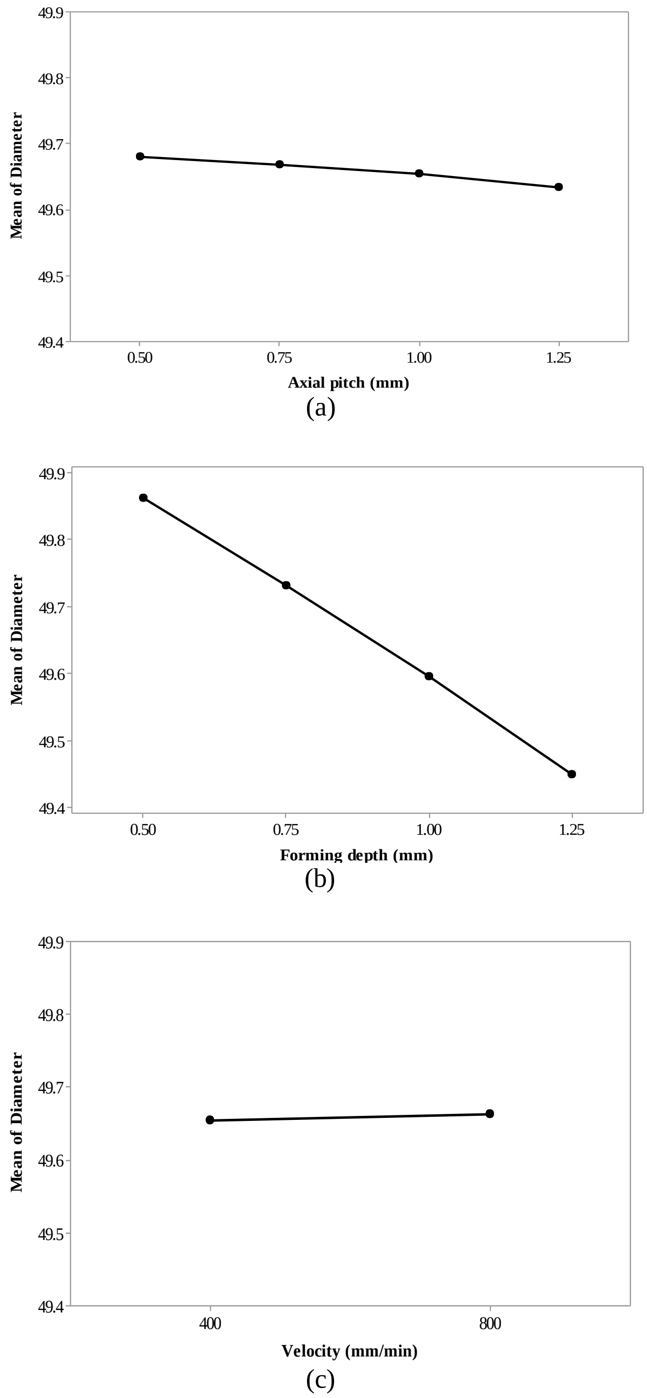

Fig. 7. Effect of input parameters on bulge diameter, a) axial pitch, b) forming depth, c) velocity

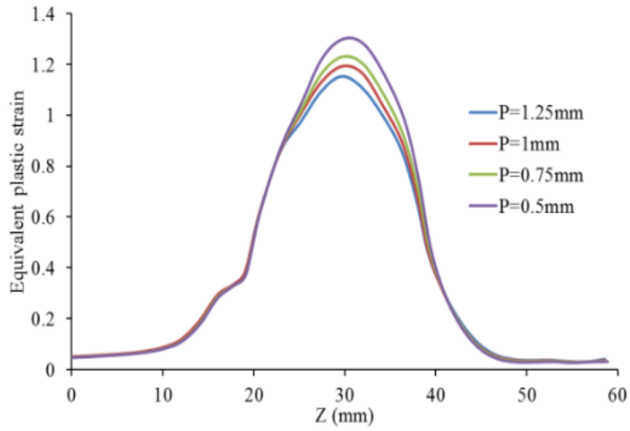

(a)

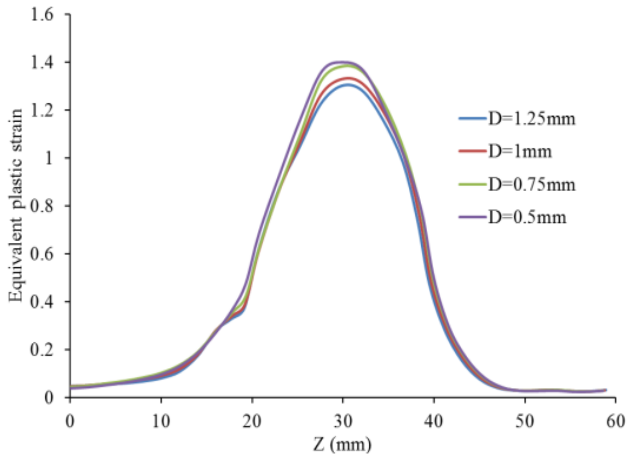

(b)

Fig. 8. Distribution of plastic strain along the longitudinal direction; (a) Different forming pitches with 1.25mm forming depth, (b) Different forming depths with a 0.5mm axial pitch

The plastic strain distribution along the longitudinal direction for different forming depths with 0.5 mm axial pitch and 800 mm/min velocity is shown in Figure 8(b). As the forming depth increases, the amount of plastic strain decreases, resulting in a larger spring-back. For this reason, smaller bulge diameter is obtained for specimens with higher forming depth. Variations of the equivalent plastic strain in an element in the middle of the tube for different forming depths with constant velocity and pitch are shown in Figure 9. As the forming depth increases, the plastic strain increases per pass, but the total strain created in all passes is less. In fact, the elastic strain and hence the spring-back increase with the increase of the forming depth, resulting in lower bulge height.

The interactions of the forming depth and the axial pitch on the bulge diameter is shown in Figure 10. It is shown that the minimum pitch and depth should be used to achieve the highest bulge diameter.

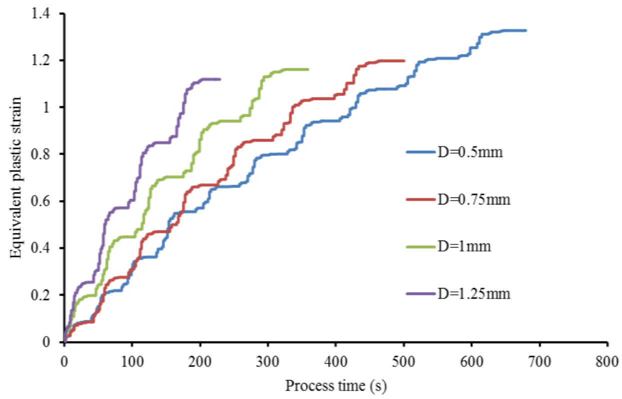

Fig. 9. Plastic strain variations in the middle of tube for 0.5mm axial pitch and 800 mm/min velocity

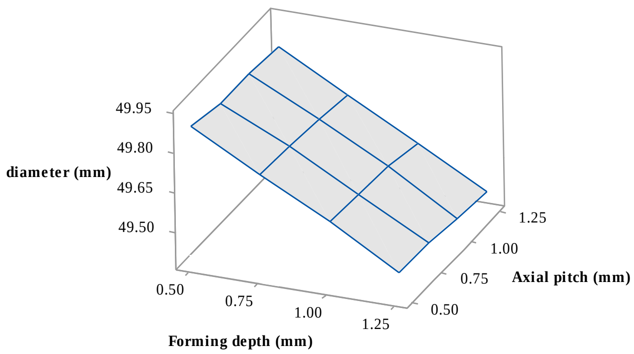

Fig. 10. Interactions of forming depth and axial pitch on the bulge

The main effect plots of input parameters on the tube length is shown in Figure 11. It is clear that the increase of axial pitch increases the tube length, but the higher forming depth results in length reduction. Large forming depth, especially in the first and last rounds of the tool rotation in each pass, causes the tube to be pulled into the forming zone. By increasing the axial pitch and decreasing the contact length, the amount of tube flow into the forming zone will be reduced and the final length will be higher. Again, the process velocity had an insignificant effect on the final tube length.

The interaction between the axial pitch and forming depth on the tube length is shown in Figure 12. It shows that the maximum axial pitch and the minimum forming depth will cause the specimen to form the maximum length.

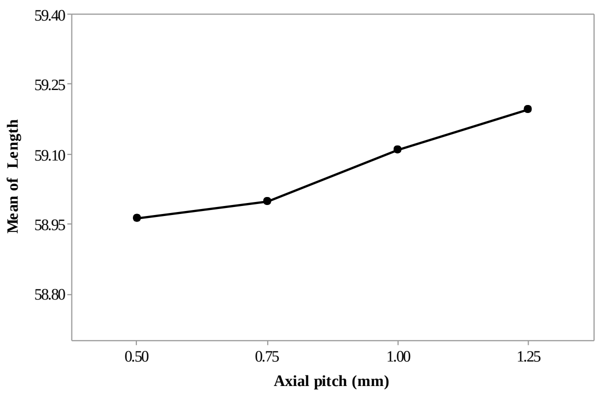

(a)

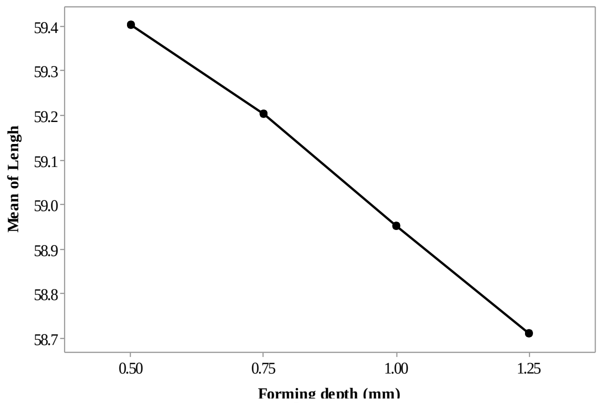

(b)

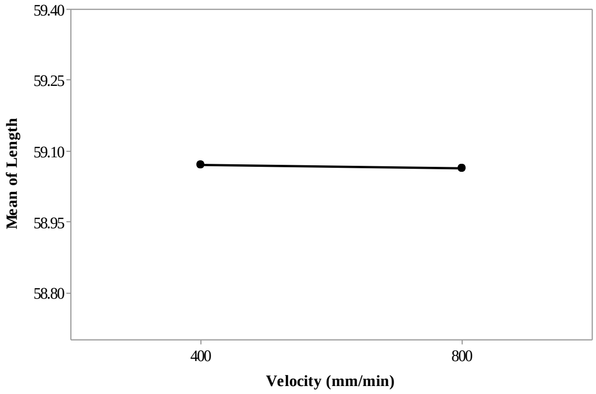

(c)

Fig. 11. The main effect plots of input parameters on the tube length; a) axial pitch, b) forming depth, c) velocity

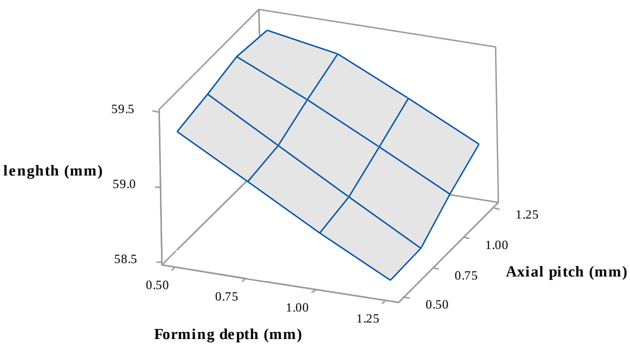

Fig. 12. Interaction of forming depth and axial pitch on the final tube length

4. CONCLUSIONS

In this paper, the incremental forming of AA6063 aluminum tubes is investigated numerically and experimentally. Axial symmetric expansion was performed in the middle of the tube without involvement of any dies. Effects of process parameters such as forming depth, axial pitch and tool linear velocity on dimensional accuracy of the components were studied. The results showed that the forming depth is the main parameter in the process. The forming velocity did not have a significant effect on the final bulge diameter and length of the specimens. Increasing the axial pitch will reduce the plastic strain resulting in a larger spring-back and eventually lower bulge diameter. The forming depth has a similar effect on the bulge diameter. Increasing the forming depth causes the material to be pulled from the die into the forming zone, and so the final length is reduced. The maximum sample length is created when the most axial pitch is used.

5. REFERENCES

1. Ambrogio, G., Costantino, I., De Napoli, L., Filice, L., Fratini, L., Muzzupappa, M., (2004). *Influence of some relevant process parameters on the dimensional accuracy in incremental forming: a numerical and experimental investigation*, J. Mater. Process. Technol., **153**, 501-507.
2. Asghar, J., Lingam, R., Shibin, E., Reddy, N. V., (2014). *Tool path design for enhancement of accuracy in single-point incremental forming*, Proc. Inst. Mech. Eng. B. J. Eng. Manuf., **228**(9), 1027-1035.
3. Attanasio, A., Ceretti, E., Giardini, C., (2006). *Optimization of tool path in two points incremental forming*, J. Mater. Process. Technol., **177**(1-3), 409-412.
4. Attanasio, A., Ceretti, E., Giardini, C., Mazzoni, L., (2008). *Asymmetric two points incremental forming: improving surface quality and geometric accuracy by tool path optimization*, J. Mater. Process. Technol., **197**(1-3), 59-67.
5. Bambach, M., (2008). *Process strategies and modelling approaches for asymmetric incremental sheet forming*. PhD Dissertation, Umformtechnische Schriften.
6. Bambach, M. B., Araghi, T., Hirt, G., (2009). *Strategies to improve the geometric accuracy in asymmetric single point incremental forming*, J. Prod. Eng., **3**(2), 145-156.
7. Behera, A. K., Vanhove, H., Lauwers, B., Duflou, J. R., (2011). *Accuracy improvement in single point incremental forming through systematic study of feature interactions*, Key Eng. Mater., **473**, 881-888.
8. Behera, A. K., Verbert, J., Lauwers, B., Duflou, J. R., (2013). *Tool path compensation strategies for single point incremental sheet forming using multivariate adaptive regression splines*, Comput. Aided Des., **45**(3), 575-590.
9. Cristino, V. A., Magrinho, J. P., Centeno, G., B. Silva, M., Martins, P. A. F., (2020). *Theory of single point incremental forming of tubes*, J. Mater. Process. Technol., 116659.
10. Duflou, J. R., Callebaut, B., Verbert, J., De Baerdemaeker, H., (2007). *Laser assisted incremental forming: formability and accuracy improvement*, CIRP Annals, **56**(1), 273-276.
11. Ham, M., Jeswiet, J., (2008). *Dimensional accuracy of single point incremental forming*, Int. J.

Mater. Form., **1**, 1171-1174.
12. Khalifa, N. B., Thiery, S., (2019). *Incremental sheet forming with active medium*. CIRP Annals, **68**(1), 313-316.
13. Leszak, E., *Apparatus and process for incremental dieless forming* USA Patent 3,342,051, issued September 19, 1967.
14 Lingam, R., Bansal, A., Reddy, N. V., (2016). *Analytical prediction of formed geometry in multi-stage single point incremental forming*, Int. J. Mater. Form., **9**(3), 395-404.
15. Malhotra, R., Xue, L., Belytschko, T., Cao, J., (2012). Mechanics of fracture in single point incremental forming. J. Mater. Process. Technol., **212**(7), 1573-1590.
16. Martins, P., Bay, N., Skjødt, M., Silva, M., (2008). *Theory of single point incremental forming*, CIRP Annals, **57**, 247-252.
17. Micari, F., Ambrogio, G., Filice, L., (2007). *Shape and dimensional accuracy in single point incremental forming: state of the art and future trends*, J. Mater. Process. Technol., **191**(1-3), 390-395.
18. Movahedinia, H., Mirnia, M. J., Elyasi, M., Baseri, H., (2018). *An investigation on flaring process of thin-walled tubes using multistage single point incremental forming*, Int. J. Adv. Des. Manuf. Technol., **94**(1-4), 867-880.
19. Rahmani, F., Seyedkashi, S. M. H., Hashemi, S. J., (2019). *Experimental investigation of converting circular tubes into square cross-sectional parts using incremental forming process*, Trans. Nonferrous Met. Soc. China, **29**(11), 2351-2361.
20. Raujol-Veillé, J., Toussaint, F., Tabourot, L., Vautrot, M., Balland, P., (2015). *Experimental and numerical investigation of a short, thin-walled steel tube incremental forming process*, J. Manuf. Process., **19**, 59-66.
21. Seyedkashi, S. M. H., Moslemi Naeini, H., Liaghat, G. H., Mosavi Mashadi, M., Mirzaali, M., Shojaee, K., Moon, Y. H., (2012a). *The effect of tube dimensions on optimized pressure and force loading paths in tube hydroforming process*, J. Mech. Sci. Technol., **26**(6), 1817-1822.
22. Seyedkashi, S. M. H., Moslemi Naeini, H., Liaghat, G. H., Mosavi Mashadi, M., Shojaee, K., Mirzaali, M., Moon, Y. H., (2012b). *Experimental and numerical investigation of an adaptive simulated annealing technique in optimization of warm tube hydroforming*, P. I. Mech. Eng. B-J. Eng. Manuf., **226**(11), 1869-1879.
23. Seyedkashi, S. M. H., Ghiri, S. J., Rahmani, F., (2017). *Experimental investigation of effective parameters on a new incremental tube bulging method using rotary tool*, Int. J. Adv. Des. Manuf. Technol, **10**(2), 83-91.
24. Teramae, T., Manabe, K., Ueno, K., Nakamura, K., Takeda, H., (2007). *Effect of material properties on deforming behavior in incremental tube-burring process using a bar tool*, J. Mater. Process. Technol., **191**(1-3), 24-29.
25. Tong, W., Yang, C., Zhang, S., Liu, L., (2015). *Characterization of deformation behavior of thin-walled tubes during incremental forming: a study with selected examples*, Int. J. Adv. Manuf. Technol., **78**(9-12), 1769-1780.
26. Yang, C., Wen, T., Liu, L. T., Zhang, S., Wang, H., (2014). *Dieless incremental hole-flanging of thin-walled tube for producing branched tubing*, J. Mater. Process. Technol., **214**(11), 2461-2467.

Received: October 02, 2020 / Accepted: December 15, 2020 / Paper available online: December 20, 2020